

Retrieval of reflections from ambient-noise field data using illumination diagnostics

Carlos Almagro Vidal*, Joost van der Neut, Deyan Draganov, Guy Drijkoningen and Kees Wapenaar, Delft University of Technology

SUMMARY

Seismic interferometry (SI) enables the retrieval of virtual-shot records at the location of receivers. In the case of passive SI, no active sources are required for the retrieval of the reflection response of the subsurface, but ambient-noise recording only. It is the illumination features of the recorded ambient noise that determine the resulting retrieved response.

Such characteristics, like geometry and signature of the noise sources, together with the complexity of the medium, are responsible for the quality of the retrieved virtual-shot events and the length of the recorded noise. To retrieve body-wave reflections, one would need to correlate body-wave noise from relatively deeper sources. A source of such noise might be the regional seismicity. In regions with noticeable human presence, the dominant noise sources will be located at or close to the surface. In the later case, the noise will be dominated by surface waves and consequently also the retrieved virtual-shot records will contain retrieved surface waves drowning retrieved reflections.

We present a method for carrying out an illumination diagnostics of the recorded ambient noise using the correlation results from the recorded noise. We explain the method using an example from a passive dataset recorded at Annerveen, Northern Netherlands, and show how this diagnostic tool helps improve the retrieval of reflections.

INTRODUCTION

Seismic interferometry (SI) enables the retrieval of the impulse response (Green's function) between receivers as if one of them were a virtual source. Schuster (2009) gives an overview of how using data from either active or passive sources one can retrieve the Green's function using a correlation, convolution or deconvolution processes. Passive SI requires only (crosscorrelation of) ambient-noise records in order to retrieve the reflection response of the subsurface. The quality of the retrieved response depends on the characteristics of the noise and the source distribution (together with the complexity of the medium), and the recording time length.

Shapiro and Campillo (2004) demonstrated how crosscorrelation of ambient noise successfully retrieves surface waves. Draganov et al. (2009) showed how reflection events were retrieved after suppressing the dominant surface-wave noise. When ambient noise consists of predominant surface-wave noise, generated by sources close to or at the Earth's surface, the retrieved results will exhibit surface waves that will drown out the retrieved weaker reflections. In order to retrieve the reflection events, suppression of the surface waves becomes a goal. One possibility is to apply the suppression to the recorded noise. Even when reflections are retrieved, they might not be obtained

correctly due to preferential illumination of the recording array with body waves from certain directions.

This method is applied to ambient noise recorded in the North of the Netherlands, in a location near the town of Annerveen. The acquisition geometry consists of two line arrays of receivers, one perpendicular to the other, as displayed in Figure 1. The first line has a NE orientation and is composed of 40 receivers equally spaced at 12 m. The second line follows a NW orientation and has 10 receivers with 48 m spacing. Both arrays are buried at 50 m depth in the ground. The recording time sampling is 2 ms. A total of 2 hours and 5 minutes of ambient noise has been processed for this work, split into 1501 time windows, of 10 s length and 5 s overlap between each other.

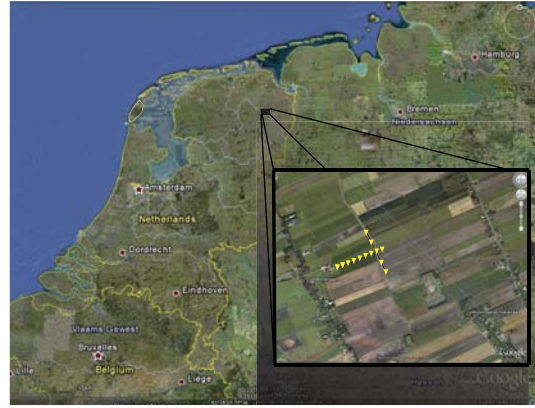


Figure 1: Geographical location of Annerveen, Northern Netherlands, where the noise was recorded. In the zoomed-in part, the two receiver lines are displayed, one perpendicular to the other. The number of receivers and their spacing are different in both lines: the NE line has 40 receivers, while the NW one only 10; the spacings are 12 m and 48 m, respectively.

METHOD

For simultaneously acting noise sources, Wapenaar and Fokkema (2006) introduce a relation to retrieve the Green's function $G(\mathbf{x}_A, \mathbf{x}_B, \omega)$ between a receiver at \mathbf{x}_A and a virtual source at \mathbf{x}_B from recordings at these two points:

$$\Re \{ \hat{G}(\mathbf{x}_A, \mathbf{x}_B, \omega) \} \hat{S}_0(\omega) \approx \frac{1}{\rho c} \left\langle \left\{ \hat{p}^{obs}(\mathbf{x}_A, \omega) \right\}^* \hat{p}^{obs}(\mathbf{x}_B, \omega) \right\rangle, \quad (1)$$

where \Re stands for real part, ρ and c are the constant mass density and velocity, respectively, of the medium at the position of

Retrieval of reflections from ambient-noise field data using illumination diagnostics

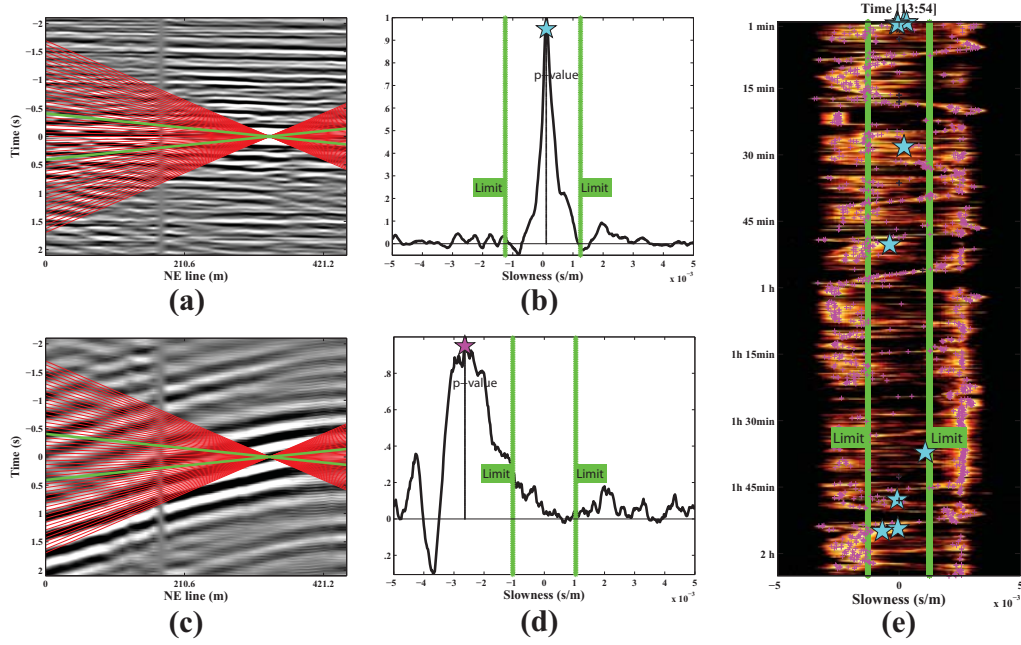


Figure 2: (a) Correlation panel for a part of the noise dominated by body-wave noise. (b) The slowness-distribution diagram for (a). The red lines indicate slownesses, while the green lines indicate limits between body-wave and surface-wave events in the virtual-source function. (c) as in (a), but for a part dominated by surface-wave noise. (d) as in (b), but for the panel in (c). (e) A succession of slowness-distribution diagrams with correlation panels that are discarded (pink stars) and those that are kept (blue stars).

the noise-sources boundary, and ω is the angular frequency; the asterisk denotes complex conjugation; the noise sources are assumed uncorrelated and with an equal power spectrum; $\hat{p}^{obs}(\mathbf{x}_A, \omega)$ stands for the total recorded noise at \mathbf{x}_A due to all the noise sources, and $\langle \cdot \rangle$ denotes spatial ensemble average. For field applications, the ensemble average is exchanged for summation over time windows.

The correlation in the right-hand side of equation 1 for one virtual source (at \mathbf{x}_B) and a number of receivers (at \mathbf{x}_A) gives a correlation panel with causal and acausal parts. Van der Neut et al. (2011) showed that the events in this gather that pass through $t = 0$ s and the position of the virtual source are an approximation of the point-spread function, which, in its turn, is informative of the illumination characteristics of the sources in the medium. They call the collection of these events the virtual-source function.

This work has no further intention to make use of the virtual-source function than to analyze the illumination information it brings in relation to each correlation panel. For further applications of the virtual-source function, the readers are referred to Wapenaar and van der Neut (2010).

In continuous noise recordings the virtual-source function is dependent on the noise sources acting during the recording time. Evaluation of the virtual-source function for a relatively

short time window would diagnose the illumination characteristics of the noise sources active during that time window. Virtual-source functions from the correlation panel of each ambient-noise time window show the illumination characteristics of each of these windows. The extracted characteristics could be used to decide if a correlation panel, that is the averaged argument in equation 1, from a certain time window would contribute to the retrieval of mainly body waves or of mainly surface waves, and therefore be kept or discarded, respectively.

The virtual-source function opens a variety of techniques for the study of the illumination characteristics of the correlated panels. One possibility is the use of the frequency-wavenumber domain and the study of the energy distribution along different velocities. A second alternative is the use of slant-stack or $\tau - p$ transform to the virtual-source panel. That is, for the time-domain u field:

$$\tilde{u}(\tau, p) = \int u(\tau + px, x) dx. \quad (2)$$

Compared to the frequency-wavenumber approach, this representation has the advantage of being less time demanding as it does not require any Fourier transform. In the correlation panel, the events in the virtual-source function are summed along slownesses taken to pass through the time origin ($\tau = 0$). Figure 2 shows the result of applying the $\tau - p$ analysis to

Retrieval of reflections from ambient-noise field data using illumination diagnostics

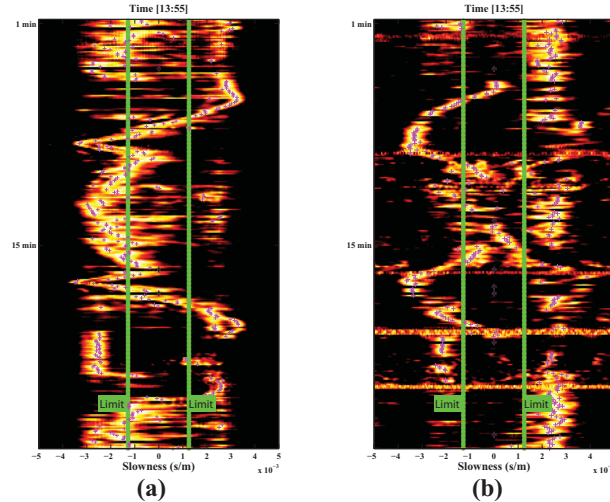


Figure 3: **(a)** The first half-an-hour part of the slowness distribution diagram in Figure 2e for the NE line. **(b)** As in (a), but for the NW line. The stars indicate the maximum of the slowness distribution for each of the correlated panels. The pink color of the stars signifies that all panels have been judged to be unsuitable to retrieval of reflection arrivals. Between minutes 5 and 20 one can identify a helix feature in the slowness distribution.

two different correlated panels from the ambient-noise recordings. Figure 2a illustrates both causal and acausal parts of a correlated panel, with the source function in the middle, for a noise time window dominated by body waves. Figure 2c represents a correlation panel from a noise time window dominated by surface waves. The red lines represent slownesses or p-values that are analyzed at the source function for $\tau = 0$. The obtained slowness analysis are stacked and the resulting slowness-distribution diagrams are displayed in Figures 2b and 2d. To use the diagram for discrimination between body-wave and surface-wave energy, we define as a limit for surface-wave detection a velocity of 800 m/s (represented by the green lines in Figure 2). If the maximum of a diagram is at a slowness value between the defined limits, as is the case in Figure 2b, then the concerned correlation panel is kept for further use in the summation process of the correlation results for the retrieval of a virtual-source gather. For the case in Figures 2c and 2d, the dominant slowness is that of surface waves and because of this the correlation panel will not be selected for further use in the summation process of the correlated panels. For a continuous recording, calculation of slowness-distribution diagrams for successive time windows allows the build up of a panel (Figure 2e) that illustrates which correlated time windows are suitable for retrieval of reflections and which are not.

Almagro Vidal et al. (2011) show the application of this diagnostic method to 2D numerically modeled data from both transient and white-noise sources.

For applications of the diagnostic tool to field ambient noise, evaluation of the illumination characteristics only along one line is not sufficient for discrimination between surface-wave and body-wave energy. For unambiguous characterization of an event as being a body-wave noise, one would need ambi-

ent noise recorded along two (perpendicular) lines. In Figure 3a, we can see that several correlated time windows of ambient noise are dominated by arrivals with low slowness values, which fall inside the limits for being characterized as body-wave noise. Nevertheless, the slowness panel in Figure 3b, shows us that these events are surface waves as for these same time windows, the NW line is dominated by high slowness values, that is by surface-wave noise. Therefore, only correlated panels from time windows that are dominated by low slowness values on the diagrams for both the NE and NW lines are being selected for the consecutive summation of the correlated noise time windows.

RETRIEVAL OF REFLECTIONS FROM THE RECORDED NOISE

Figures 4a and 4b show the retrieved common-source gather for a virtual source at the position where both lines are crossing each other. The results are obtained after summing all 1501 correlated panels along the NE and NW lines, respectively, and adding time-reversed acausal parts to causal parts of the summed correlated functions. The results exhibit only retrieved surface waves. Figure 2e shows the slowness distribution of all correlated time windows as recorded along the NE line: this demonstrates the nearly total dominance of energy in the noise with surface-wave slownesses. From the total amount of 1501 correlated panels, only 10 contain predominant body-wave noise. Five of the later windows are from the first analyzed minute of noise and represent a small earthquake that happened at that time. Note that, as explained in the previous section, the decision if an event in a noise time window represents a body wave is taken by using in conjunction the

Retrieval of reflections from ambient-noise field data using illumination diagnostics

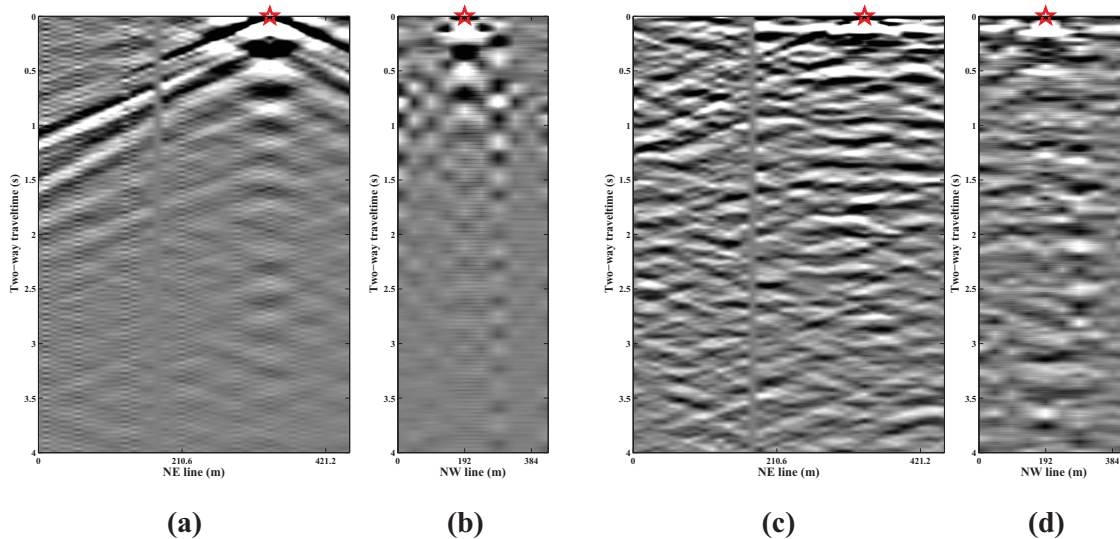


Figure 4: **(a)** Virtual-source gather along the NE line. This result was obtained from the correlation and summation of all analyzed 1501 time windows. We see in it only retrieved surface waves. **(b)** As in (a), but along the NW line. **(c)** as in (a), but after the illumination diagnostics and elimination from the summation process of correlated panels that are dominated by surface waves. **(d)** as in (b), after the illumination diagnostics. The virtual source, represented by the red star, is at 348 m, at which point the two lines are crossing each other.

slowness panels for both perpendicular lines.

Figures 4c and 4d display the SI retrieval result from summing only the correlated panels that were classified by our method to be dominated by body-wave noise. We can observe that surface waves are suppressed, while flat events have been brought forward. Such events, like the ones at 0.2 s, 0.5 s, 0.9 s, 1.3 s for example, are potentially retrieved reflection arrivals. Nevertheless, some of these arrivals might be non-physical too. Move-out features are poorly retrieved due to the lack of additional illumination angles, as the time windows selected for the summation process are dominated by body-wave noise with low slownesses. Increased illumination of the recording lines by body-wave noise could contribute, in addition to potential retrieval of wings of retrieved reflection hyperbolae, the suppression of non-physical arrivals by destructive interference.

The limited illumination that we observe comes from two factors. The first one is the limited amount of analyzed recorded noise. We expect that after analyzing much longer noise, we would obtain more time windows dominated by body-wave energy. The second reason is that the analysed part of the noise is recorded during the afternoon hours. During these hours, there is a lot of human-activity noise, which produces strong surface-wave energy. The slowness analysis in Figures 3a and 3b shows such noise - the sinusoidal character of the dominant slowness in both panels indicates a moving noise source, possible a tractor used for farming the field.

CONCLUSIONS

We proposed a method to analyze the illumination characteristics of recorded ambient noise to be used for passive seismic interferometry. In our method, we used events in the correlated noise windows that pass through the virtual-source position at zero time. We transformed these events to the slowness domain and analyzed them to classify the different noise windows as being dominated by surface waves or by body waves. We applied the analysis to ambient noise recorded at Annerveen, The Netherlands. We showed that by not using noise windows, classified as dominated by surface waves, the result from seismic interferometry exhibited possible retrieved reflections. Thus, the proposed method enables the exclusion of correlated noise with dominant surface waves, but also allows concentration of useful information, discarding unnecessary data and reducing processing and storage costs.

ACKNOWLEDGMENTS

This work is supported by the Netherlands Research Centre for Integrated Solid Earth Science (ISES) and the Dutch Technology Foundation STW.